**FULL PAPER**

ADVANCED
OPTICAL
MATERIALS

www.advopticalmat.d

Check for updates

# Photoinduced Trap Passivation for Enhanced Photoluminescence in 2D Organic–Inorganic Hybrid Perovskites

*Yiling Song, Weiwei Liu,\* Yan Qin, Xiaobo Han, Wancai Li, Xiaohong Li, Hua Long, Dehui Li, Kai Wang, Bing Wang, and Peixiang Lu\**

2D organic–inorganic hybrid perovskites are promising materials for next-generation optoelectronic devices. Nevertheless, 2D perovskites still suffer from performance-limiting trap states and possess fundamental photophysical effects that remain poorly understood. Herein, a photoinduced trap passivation for enhanced photoluminescence (PL) in 2D hybrid perovskites is reported. Under two-photon excitation, the PL emission of the 2D hybrid perovskites exhibits a gradual increase in intensity and lifetime, due to the photoinduced trap passivation by interacting with oxygen in ambient environment. Interestingly, the PL increase shows distinct features at the surface and in the bulk of the 2D perovskites, which can be well revealed by a photoinduced oxygen-diffused trap-passivation model. Moreover, the PL increase and relaxation can recycle for several times, which suggests an excellent repeatability of the photoinduced trap passivation. The photoinduced trap passivation is critical for fundamental study of light–matter interaction in 2D perovskites, and shows great promise for improving the optoelectronic responses for functional devices.

## 1. Introduction

Driven by the remarkable optoelectronic properties, hybrid perovskites have shown great promise for high-performance functional devices including solar cells,[1–3] light-emitting diodes,[4,5] and photodetectors.[6,7] In particular, organic–inorganic perovskites have opened up a new territory of solar cells with power conversion efficiency over 25%.[8] As an excellent candidate for optoelectronics, photoinduced effects in organic–inorganic perovskites have attracted increasing

attentions due to serious concerns on the stability and lifetime of the optoelectronic devices.[9–12] For examples, photoinduced trap filling has been demonstrated to be responsible for reducing trap density in organic–inorganic perovskites.[13] In addition, photoinduced reaction and ionic immigration are helpful for healing the trap states in hybrid perovskites.[14–16] Despite great advantages, lightinduced performance degradation of the hybrid perovskites still remains a significant challenge for high-performance optoelectronic devices.[10,17,18]

More recently, 2D organic–inorganic hybrid perovskites with a layered multi-quantum-well structure, have been demonstrated to possess more outstanding properties, such as a larger exciton binding energy,[19,20] a greater tunability,[21–24] and a better stability.[25,26] Encouraged by the impressive features, 2D perovskites have become potential candidates for next-generation optoelectronic devices like high-efficiency light emitting devices and high-performance solar cells.[27–29] Besides, 2D perovskites also provide an excellent platform for novel photophysics, such as edge states and Stark effect.[21,30–33] Although showing great promise for functional applications, photoinduced structural changes, and physical effects in 2D perovskites still remains elusive. Therefore, a deep insight into the photoinduced effects in 2D hybrid perovskites is of critical importance for revealing the light-matter interaction mechanism and improving the performances of optoelectronic devices.

In this work, we report a novel photoinduced photoluminescence (PL) enhancement in the single crystals of 2D organic–inorganic perovskites under two-photon excitation. The two-photon absorption induced photoluminescence (TPL) of 2D perovskite flakes displays a gradual increase over time, up to ≈3.7 times of the initial intensity. By using in situ techniques, such as scanning electron microscopy (SEM) and micro-photoluminescence (μ-PL) spectroscopy, the PL enhancement is correlated to trap passivation at the surface and in the bulk of the perovskite flakes. The interaction dynamics can be well revealed by a photoinduced oxygen-diffused trap-passivation model. Moreover, reversibility measurement results indicate that the photoinduced trap passivation can be reactivated for several cycles and exhibits an excellent repeatability. In addition, a photoinduced carrier diffusion in the 2D layered perovskite is observed, showing a large diffusion distance over 10 μm.

Y. Song, Dr. W. Liu, Y. Qin, X. Li, Dr. H. Long, Prof. K. Wang,
Prof. B. Wang, Prof. P. Lu
Wuhan National Laboratory for Optoelectronics
Huazhong University of Science and Technology
Wuhan 430074, China
E-mail: lwhust@hust.edu.cn; lupeixiang@hust.edu.cn
Dr. X. Han, Prof. P. Lu
Hubei Key Laboratory of Optical Information and Pattern Recognition
Wuhan Institute of Technology
Wuhan 430205, China
W. Li, Prof. D. Li
School of Optical and Electronic Information
Huazhong University of Science and Technology
Wuhan 430074, China

**1901695** (1 of 7)

## 2. Results and Discussion

$(PEA)_2PbI_4$ monocrystalline films were synthesized using an antisolvent vapor-assisted capping crystallization method.[34,35] After that, the 2D perovskite flakes were mechanically exfoliated onto polydimethylsiloxane substrates with a scotch tape. The $(PEA)_2PbI_4$ flakes were characterized with SEM and X-ray diffraction (XRD), respectively (Figures S1 and S2, Supporting Information). Optical measurement was performed on an μ-PL system (Figure S3, Supporting Information), in which the laser beam from a femtosecond Ti-sapphire oscillator (800 nm, 30 fs, 80 MHz) was used for excitation. As the photon energy of the femtosecond laser pulses is much smaller than the bandgap of the 2D perovskite (≈2.274 eV), the electrons can transit by a simultaneous absorption of two low-energy photons (Figure S4, Supporting Information).[32,36–38] More importantly, the near-infrared photons are nearly transparent to the 2D perovskite in linear-absorption regime, thus preventing the photoinduced degradation of the layered perovskite. **Figure 1**a shows the dark-field images of the TPL emission captured at different times under continuous excitation, which clearly present an enhancement of the PL intensity. To quantitatively characterize the evolution, the TPL spectra were monitored by a spectrometer (Andor 193i), as plotted in Figure 1b. The PL intensity shows a rapid increase in the first 100 s, and gradually becomes stable to ≈3.7 times of the initial intensity. Moreover, the 2D pseudocolor plot of the time-dependent TPL spectra (Figure 1c) presents unchanged spectrum shape and emission peak, suggesting that the source of the PL emission remains to be exciton recombination in the 2D perovskite.

The micromorphology and element distribution of the irradiated area were characterized by SEM and energy dispersive spectrum (EDS), respectively. **Figure 2**a shows that the irradiated area displays a bright spot in the SEM image, corresponding to a microstructure produced by the femtosecond laser irradiation (inset of Figure 2a). The EDS of the irradiated area shown in Figure 2b indicates that besides the intrinsic elements of the organic–inorganic perovskite, oxygen appears in the sample, which may be due to the oxygen adhered onto the crystal surface.[39] Oxygen-related species could deactivate the trapping sites and improve the optical responses of the organic–inorganic perovskites, which played important roles for the photoinduced PL enhancement in 3D perovskites.[15,39–42] For further demonstration, the PL properties of the 2D perovskite flakes were measured in vacuum ($6 \times 10^{-2}$ Pa) and in ambient environment, respectively. Figure 2c shows an increased PL intensity in ambient environment compared with that in vacuum, indicating that the ambient atmospheres have indeed contributed to the PL enhancement in the 2D perovskite. Furthermore, the PL variation traces in Figure 2d shows that the PL enhancements in ambient environment and in oxygen are larger than that in vacuum. We also investigated the influence of the other gases, whose effect on the PL enhancement can be excluded (Figures S6 and S7, Supporting Information). Therefore, the comparison demonstrates that oxygen has played a dominant role for the photoinduced PL enhancement of the 2D perovskite. As reported, exposure to light and oxygen will lead to the formation of a superficial layer of negatively charged oxygen species on the surface of the organic–inorganic hybrid perovskites, which is capable of deactivating the trap states by repelling the defects away from the surface.[39] As a result, PL emission can be enhanced due to the reduction of trapinduced nonradiative recombination.

We measured time-resolved transient PL (TRPL) to investigate the recombination dynamics in the 2D perovskite flake under light irradiation. **Figure 3**a plots the TRPL decay traces measured over time, which shows that the average PL lifetime increases from 2.17 to 2.93 ns after 900 s. The increased PL lifetime suggests a suppression of the nonradiative recombination in the 2D perovskite, which can be correlated to the
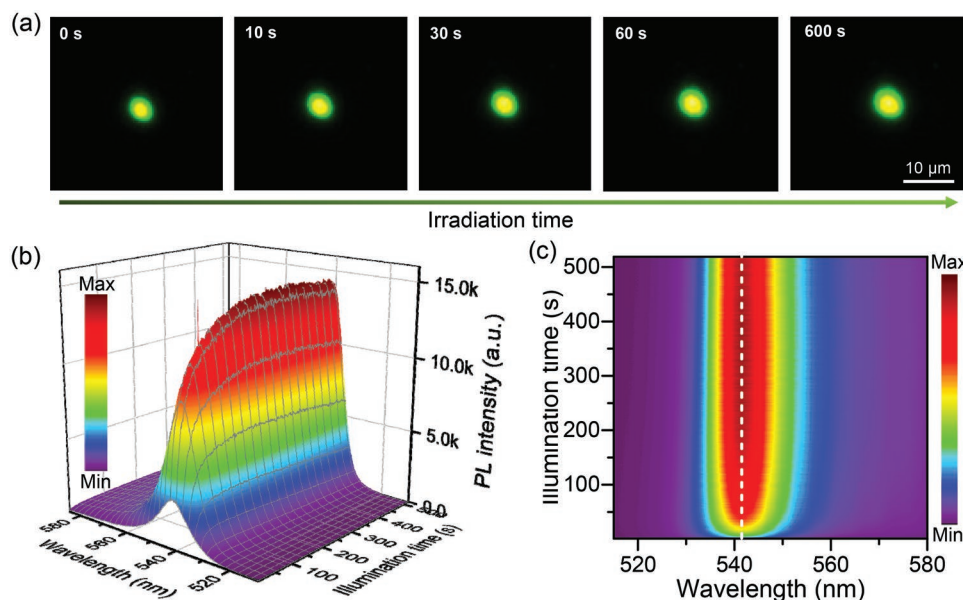


**Figure 1.** a) Dark-field images of the TPL from a $(PEA)_2PbI_4$ flake taken at different times. b) Evolution of the TPL spectra of the $(PEA)_2PbI_4$ flake as a function of time. c) 2D pseudocolor plot of the TPL spectra in (b), showing that the emission peak does not shift over time.
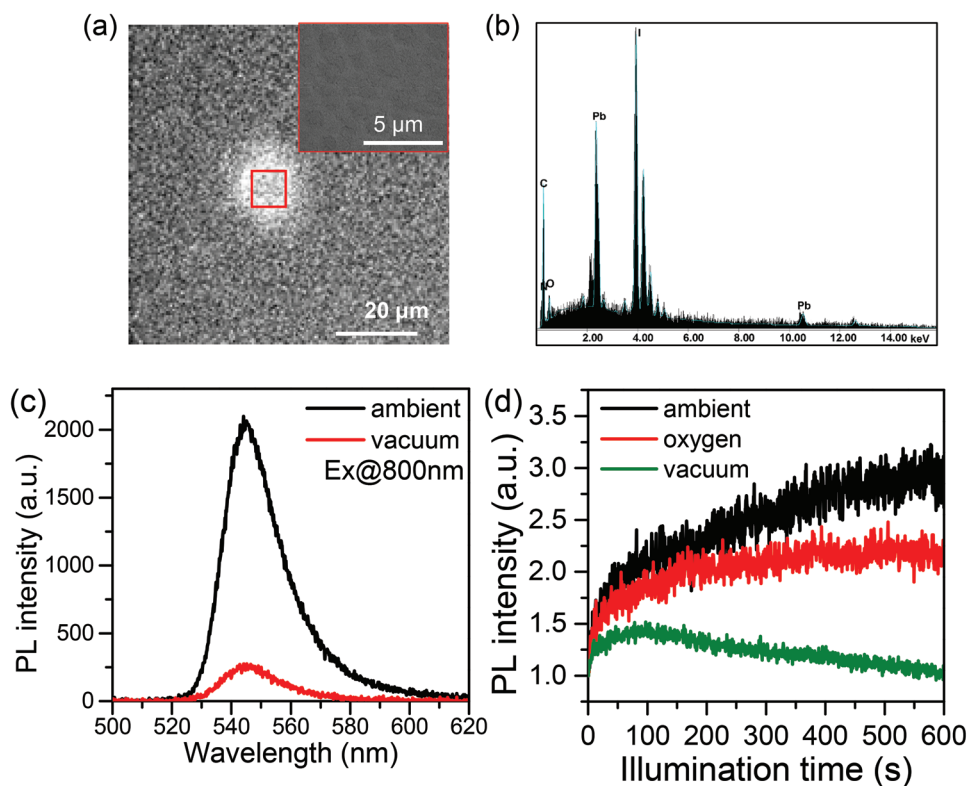
**ADVANCED
SCIENCE NEWS**
www.advancedsciencenews.com

**ADVANCED
OPTICAL
MATERIALS**
www.advopticalmat.de

**Figure 2.** a) SEM image of a irradiated $(PEA)_2PbI_4$ flake. The inset shows an enlarged present corresponding to the red rectangle. b) EDS spectrum for the irradiated area of the $(PEA)_2PbI_4$ flake. c) Initial TPL spectra of a $(PEA)_2PbI_4$ flake measured under 800 nm excitation, in ambient and in vacuum, respectively. d) Normalized TPL variation traces of the same $(PEA)_2PbI_4$ flake measured under 800 nm excitation, in ambient, pure oxygen and in vacuum, respectively.

photoinduced trap passivation effect. Power-dependent PL properties were also measured at two specific times for comparison, from the beginning of laser excitation ($t = 0$ s, A) and after the PL emission becoming stable (B). Figure 3b shows that the TPL intensity measured from $t = 0$ s (black dots) possesses a super-quadratic dependence on the excitation power ($\gamma = Ax^3$), while it becomes a normal quadratic dependence ($\gamma = Bx^2$) when the TPL emission reaches stability (red dots). In principle, the TPL intensity has a quadratic dependence on the excitation power for a normal exciton recombination under two-photon excitation.[36] However, the rapid increase of the TPL intensity over time leads to the super-quadratic dependence property at the beginning. When the trap states are fully passivated by the photoinduced effect, the TPL intensity reaches a stability and recovers to the quadratic-dependence property. The unique power-dependent properties indicate notable distinction from the mechanisms induced by trap filling and biexciton recombinations,[13,43] which provides a clear evidence for the photoinduced trap passivation in the 2D perovskite.

A deep insight into the spectrum characteristics is helpful for revealing the interaction dynamics between the perovskites and the oxygen-related species. Figure 3c (solid curves) presents the normalized TPL spectra of the $(PEA)_2PbI_4$ flake measured at different time. Interestingly, the normalized intensity of the high-energy part and low-energy part in the TPL spectra exhibit characteristics with striking contrast, which suggests that the two-part emissions originate from different sources.

Figure 3c shows that the high-energy part is overlapped with the absorption edge of $(PEA)_2PbI_4$, which will result in a strong self-absorption of the photons produced in the bulk of the perovskite flake. Therefore, the PL emission at the high-energy part is dominantly from the surface. In contrast, the PL emission at the low-energy part experiences a weak self-absorption in the perovskite flake, which represents the signal from both the surface and bulk of perovskite flake. The PL increase over the whole spectrum suggests that the trap states from both the surface and bulk of the 2D perovskite can be passivated by interacting with the oxygen-related species.

To analyze the interaction dynamics, an oxygen-diffused trap-passivation model is proposed, as illustrated in Figure 3d. In general, halogen vacancies exist in the organic metal halide perovskites, which result in shallow defects near the intrinsic band states i).[44,45] At first, the oxygen in the air will adhere to the surface of the 2D perovskite flake. Driven by the light irradiation, the oxygen-related species will interact with the shallow defects at the surface ii). As a result, the PL emission from the surface of the perovskite flake can be enhanced in a short time. Simultaneously, the laser processed microstructure on the surface of the 2D perovskite provides an excellent channel for the oxygen to diffuse into the bulk. The diffusion of oxygen will lead to a passivation of the defects inside the 2D perovskite, thus resulting in an further enhancement of the PL emission iii). As the energy levels of the shallow defects are similar to the intrinsic exciton states, the emission spectrum of
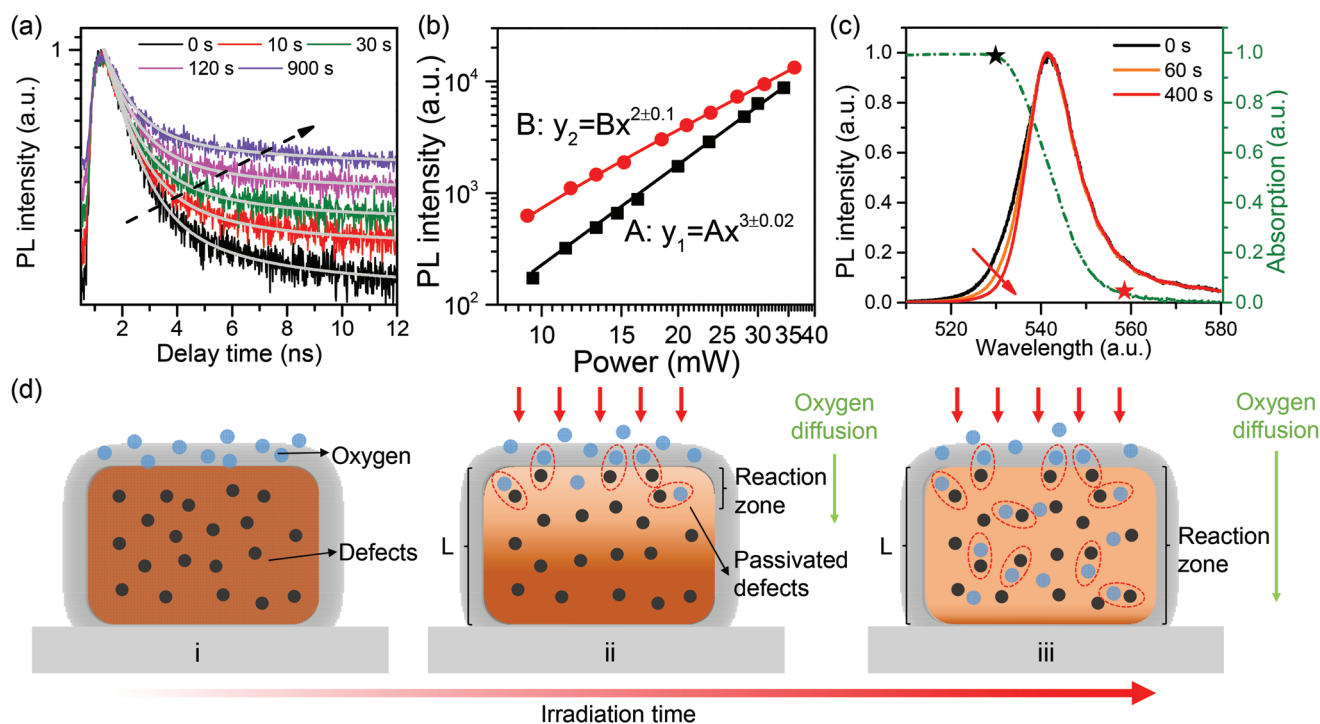
ADVANCED
SCIENCE NEWS
www.advancedsciencenews.com

ADVANCED
OPTICAL
MATERIALS
www.advopticalmat.de

**Figure 3.** a) Plot of TRPL decay traces for the $(PEA)_2PbI_4$ flake over time. b) Power-dependent TPL of the $(PEA)_2PbI_4$ flake. The results were measured at two specific times, from the beginning of laser excitation (black dots) and after the TPL emission becoming stable (red dots), respectively. c) Normalized TPL spectra of the $(PEA)_2PbI_4$ flake measured at 0, 60, and 400 s, respectively. The green dashed–dotted line presents the absorption spectrum of $(PEA)_2PbI_4$. d) Schematic for the proposed oxygen-diffused trap-passivation model.

the 2D perovskite has no obvious variation,[16] which can be well revealed by the result in Figure 1c. Considering the relative slow speed of the oxygen diffusion, the interaction inside the bulk will happen in a longer time than that at the surface. In addition, the ionic immigration and carrier diffusion in the direction vertical to the multiquantum-well plane is negligible because they are greatly depressed by the organic spacing layers.[46,47] Considering the photoinduced trap passivation with oxygen diffusion in the perovskite, the PL enhancement for the surface component can be derived as (Supporting Information)

$$\frac{I_s(t)}{I_s(0)} = \frac{1}{A + B\exp(-t/\tau_{NT1})} \tag{1}$$

while the PL enhancement for the whole part can be expressed as

$$\frac{I(t)}{I(0)} = \frac{1}{A + B\exp(-t/\tau_{NT1}) + C\exp(-t/\tau_{NT2})} \tag{2}$$

where $I_s(t)$ and $I(t)$ represent the PL intensities as a function of time. $I_s(0)$ and $I(0)$ represent the corresponding initial intensities at $t = 0$. $\tau_{NT1}$ and $\tau_{NT2}$ are the time constants for the oxygen interaction with the trap states at the surface and in the bulk of the perovskite, respectively, which are dependent on the trap passivation rate $R_{NT}$. $\tau_D$ is the time constant for the oxygen diffusion inside the perovskite.

We extracted the time-dependent PL intensity at the high-energy part (black star, 530 nm) and low-energy part (red star,

558 nm) of the PL spectra in Figure 3c, respectively, as plotted in **Figure 4**a. As analyzed above, the PL emission at 530 and 558 nm represent the signals from the surface and whole crystal of the perovskite flake, respectively. Correspondingly, the PL variation trace at 530 nm can be well fitted by Equation (1) with a time constant $\tau = 8.9$ s, while that at 558 nm can be well fitted by Equation (2), with the time constants of $\tau_1 = 9.0$ s, $\tau_2 = 75.5$ s. The good agreement between the experimental results and theoretical model provides strong evidence for the photoinduced oxygen-diffused trap-passivation model. For further demonstration, Figure 4b plots the PL variation trace of the $(PEA)_2PbI_4$ flake over time under a continuous 400 nm excitation. Due to a narrow penetration depth of single-photon excitation, only the PL from the surface of the perovskite flake can be monitored.[42,48] Figure 4b shows that the PL evolution trace can be well fitted by Equation (1), with only one time constant of $\tau = 17.4$ zs. We also measured the PL variation traces of the samples with different thicknesses, as presented in Figure 4c. The PL variation traces of a thin sample can be well fitted by Equation (1), while those of the thick samples can be well fitted by Equation (2), which also confirms the distinct interaction processes at the surface and in the bulk of the 2D perovskite flake, respectively. In addition, oxygen-concentration controlled results indicates that the interaction rates for both the surface and bulk components exhibit an increase with the oxygen concentration (Figure S9, Supporting Information), which further demonstrates the oxygen diffusion for photoinduced trap passivation.

PL mapping was performed to investigate the interaction between the perovskite flake and oxygen in the plane of the
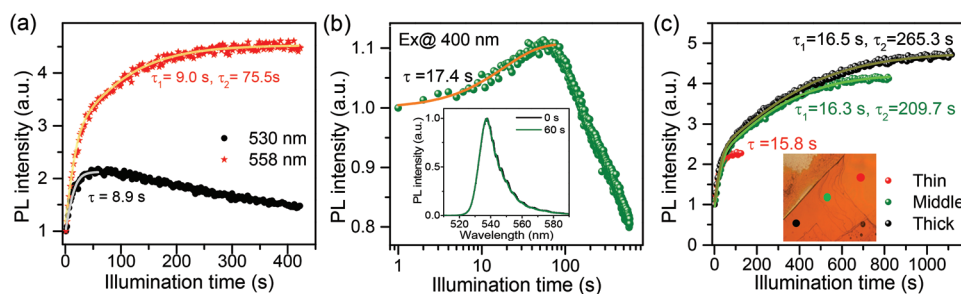
**Figure 4.** a) Normalized TPL variation trace of a $(PEA)_2PbI_4$ flake monitored at 530 and 558 nm respectively. b) Normalized PL variation trace of a $(PEA)_2PbI_4$ flake under 400 nm excitation. Inset: normalized PL spectra measured at 0 and 60 s, respectively. c) Normalized TPL variation traces for $(PEA)_2PbI_4$ flakes with different thicknesses. Inset: optical microscope image for a $(PEA)_2PbI_4$ flake with different-thickness areas.

multiquantum-well structure. The perovskite flake was continuously excited until the PL emission reaches a stability, and then the integrated PL emission around the excitation spot was probed by mapping in an area of $60 \times 60$ μm², as shown in **Figure 5**a. We can observe that the strongest PL emission is mainly from the area corresponding to the excitation spot, and the PL intensity decreases gradually as the probe position is far away from the spot center. Interestingly, the PL enhanced area is much larger than the excitation spot (diameter 15 μm). For detailed analysis, the PL intensity distribution along the crossline in Figure 5a was extracted and plotted in Figure 5b. The experimental data could be fitted to a Gaussian distribution with full width at half maximum (FWHM) of ≈21.6 μm, which implies that the photoinduced trap passivation can diffuse in the plane of the multiquantum-well structure, with a long distance over ≈10 μm. The diffusion can also be demonstrated by TRPL measurement, in which the PL lifetime exhibits a gradually decrease as the probe point gets away from the excitation spot, as shown in Figure 5c. As the photoinduced trap passivation follows a similar Gaussian distribution in space, the carrier gradient will drive the trap passivation diffusing in the lateral direction of the 2D perovskite. In addition, the influence of heating induced by the laser irradiation on the diffusion effect can be negligible (Figure S9, Supporting Information).

The reversibility of the PL enhancement was checked to characterize the relaxation dynamics of the photoinduced trap passivation process. When the PL emission of the perovskite flake reached a stability under continuous excitation, the laser was switched off for relaxing, and the PL intensity of the excited area was probed every 600 s, as shown in **Figure 6**. Without laser irradiation, the PL emission would relax and eventually

reach a new equilibrium after ≈2 h. Importantly, the PL intensity at the new equilibrium is still 2 times of the initial intensity, which indicates that the oxygen-related species can passivate the trap states for quite a long time under two-photon excitation. Moreover, the PL increase would repeat when the 2D perovskite was continuously excited again. One can observe that the PL enhancement and relaxation can recycle for several times, which suggests an excellent reversibility of the photoinduced trap passivation in ambient environment.

Besides the $(PEA)_2PbI_4$ perovskite, we also investigated the PL property of another typical 2D perovskite $((HO(CH_2)_2NH_3)_2PbI_4)$ by two-photon excitation. A similar PL increase over time under continuous excitation was observed, and the PL variation trace can be well fitted by Equation (2) (Figure S10, Supporting Information). As trap states are generally existed in the 2D perovskite crystals and nanostructures, the proposed oxygen-diffused trap-passivation model are critical for revealing the light-matter interaction mechanism of the 2D perovskites in ambient environment. Moreover, the photoinduced trap passivation provides an effective approach to improving the optoelectronic responses of the 2D perovskites.

In conclusion, we demonstrate a photoinduced trap passivation in 2D perovskite by interacting with the oxygen in ambient environment. Under two-photon excitation, the PL emission of the 2D perovskites exhibits a gradual increase in both intensity and lifetime, due to the photoinduced trap passivation in 2D perovskites. The PL increase shows distinct features at the surface and in the bulk of the 2D perovskite, which can be well revealed by the photoinduced oxygen-diffused trap-passivation model. Moreover, the photoinduced trap passivation exhibits an excellent repeatability and can be reactivated for several cycles.
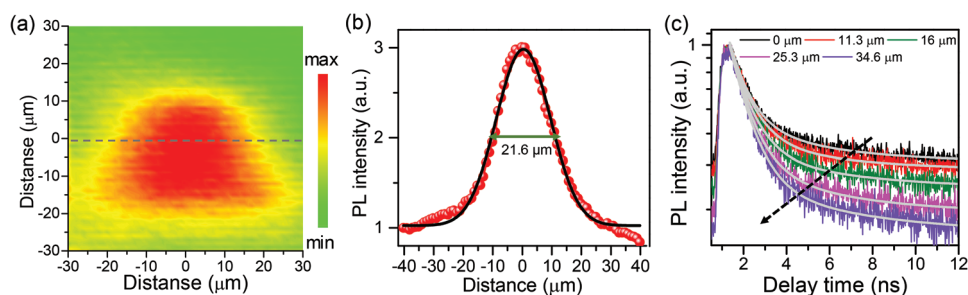


**Figure 5.** a) Integrated TPL mapping of a $(PEA)_2PbI_4$ flake. The $(PEA)_2PbI_4$ flake was irradiated to reach a stable TPL emission beforehand. b) TPL intensity distribution taken along the dashed line in (a), and the corresponding Gaussian-fitting result (black line). c) Plot of TRPL decay traces for the $(PEA)_2PbI_4$ flake as a function of the distance from the irradiated spot.
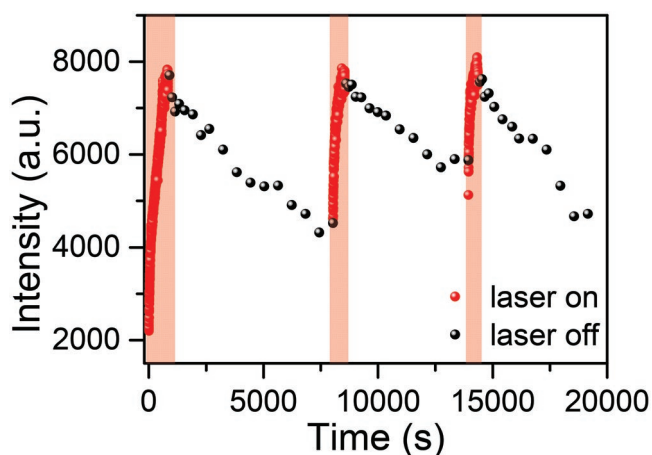
**Figure 6.** Repeatability measurement result for the trap passivation by switching on and off the irradiation laser in cycle.

The photoinduced trap passivation is critical for revealing the light-matter interaction mechanism in 2D perovskites, and shows great promise for improving the optoelectronic responses for functional devices.

## Supporting Information

Supporting Information is available from the Wiley Online Library or from the author.

## Acknowledgements

## Conflict of Interest

The authors declare no conflict of interest.

## Keywords

[1] X. Zhao, C. Yao, T. Liu, J. C. Hamill, G. O. Ngongang Ndjawa, G. Cheng, N. Yao, H. Meng, Y. L. Loo, *Adv. Mater.* **2019**, *31*, 1904494.

[2] Y. Wang, M. I. Dar, L. K. Ono, T. Zhang, M. Kan, Y. Li, L. Zhang, X. Wang, Y. Yang, X. Gao, Y. Qi, M. Grätzel, Y. Zhao, *Science* **2019**, *365*, 591.

[3] S. Bai, P. Da, C. Li, Z. Wang, Z. Yuan, F. Fu, M. Kawecki, X. Liu, N. Sakai, J. T. Wang, S. Huettner, S. Buecheler, M. Fahlman, F. Gao, H. J. Snaith, *Nature* **2019**, *571*, 245.

[4] H. Kim, L. Zhao, J. S. Price, A. J. Grede, K. Roh, A. N. Brigeman, M. Lopez, B. P. Rand, N. C. Giebink, *Nat. Commun.* **2018**, *9*, 4893.

[5] K. Lin, J. Xing, L. N. Quan, F. P. G. de Arquer, X. Gong, J. Lu, L. Xie, W. Zhao, D. Zhang, Y. Yan, W. Li, X. Liu, Y. Lu, J. Kirman, E. H. Sargent, Q. Xiong, Z. Wei, *Nature* **2018**, *562*, 245.

[6] Z. Yang, Q. Xu, X. Wang, J. Lu, H. Wang, F. Li, L. Zhang, G. Hu, C. Pan, *Adv. Mater.* **2018**, *30*, 1802110.

[7] J. Li, J. Wang, J. Ma, H. Shen, L. Li, X. Duan, D. Li, *Nat. Commun.* **2019**, *10*, 806.

[8] L. Mazzarella, Y. H. Lin, S. Kirner, A. B. Morales-Vilches, L. Korte, S. Albrecht, E. Crossland, B. Stannowski, C. Case, H. J. Snaith, R. Schlatmann, *Adv. Energy Mater.* **2019**, *9*, 1803241.

[9] A. Ummadisingu, L. Steier, J. Y. Seo, T. Matsui, A. Abate, W. Tress, M. Gratzel, *Nature* **2017**, *545*, 208.

[10] H. H. Fang, J. Yang, S. X. Tao, S. Adjokatse, M. E. Kamminga, J. T. Ye, G. R. Blake, J. Even, M. A. Loi, *Adv. Funct. Mater.* **2018**, *28*, 1800305.

[11] M. Abdi-Jalebi, Z. Andaji-Garmaroudi, S. Cacovich, C. Stavrakas, B. Philippe, J. M. Richter, M. Alsari, E. P. Booker, E. M. Hutter, A. J. Pearson, S. Lilliu, T. J. Savenije, H. Rensmo, G. Divitini, C. Ducati, R. H. Friend, S. D. Stranks, *Nature* **2018**, *555*, 497.

[12] Y. L. Song, W. W. Liu, C. Fang, D. H. Li, P. X. Lu, *Opt. Express* **2019**, *27*, 30618.

[13] S. D. Stranks, V. M. Burlakov, T. Leijtens, J. M. Ball, A. Goriely, H. J. Snaith, *Phys. Rev. Appl.* **2014**, *2*, 034007.

[14] H.-H. Fang, F. Wang, S. Adjokatse, N. Zhao, M. A. Loi, *Adv. Funct. Mater.* **2016**, *26*, 4653.

[15] Y. Tian, M. Peter, E. Unger, M. Abdellah, K. Zheng, T. Pullerits, A. Yartsev, V. Sundstrom, I. G. Scheblykin, *Phys. Chem. Chem. Phys.* **2015**, *17*, 24978.

[16] D. W. Dequilettes, W. Zhang, V. M. Burlakov, D. J. Graham, T. Leijtens, A. Osherov, V. Bulovic, H. J. Snaith, D. S. Ginger, S. D. Stranks, *Nat. Commun.* **2016**, *7*, 11683.

[17] Y. Lin, B. Chen, Y. Fang, J. Zhao, C. Bao, Z. Yu, Y. Deng, P. N. Rudd, Y. Yan, Y. Yuan, J. Huang, *Nat. Commun.* **2018**, *9*, 4981.

[18] F. Lang, O. Shargaieva, V. V. Brus, H. C. Neitzert, J. Rappich, N. H. Nickel, *Adv. Mater.* **2018**, *30*, 1702905.

[19] D. B. Straus, C. R. Kagan, *J. Phys. Chem. Lett.* **2018**, *9*, 1434.

[20] K. Wang, C. Wu, Y. Jiang, D. Yang, K. Wang, S. Priya, *Sci. Adv.* **2019**, *5*, eaau3241.

[21] J.-C. Blancon, H. Tsai, W. Nie, C. C. Stoumpos, L. Pedesseau, C. Katan, M. Kepenekian, C. M. M. Soe, K. Appavoo, M. Y. Sfeir, S. Tretiak, P. M. Ajayan, M. G. Kanatzidis, J. Even, J. J. Crochet, A. D. Mohite, *Science* **2017**, *355*, 1288.

[22] L. Dou, A. B. Wong, Y. Yu, M. Lai, N. Kornienko, S. W. Eaton, A. Fu, C. G. Bischak, J. Ma, T. Ding, N. S. Ginsberg, L.-W. Wang, A. P. Alivisatos, P. Yang, *Science* **2015**, *349*, 1518.

[23] B. Zhou, D. Yan, *Angew. Chem., Int. Ed.* **2019**, *58*, 2.

[24] S. Liu, S. S. Sun, C. K. Gan, A. G. del Aguila, Y. N. Fang, J. Xing, T. T. H. Do, T. J. White, H. G. Li, W. Huang, Q. H. Xiong, *Sci. Adv.* **2019**, *5*, eaav9445.

[25] X. Xiao, J. Dai, Y. Fang, J. Zhao, X. Zheng, S. Tang, P. N. Rudd, X. C. Zeng, J. Huang, *ACS Energy Lett.* **2018**, *3*, 684.

[26] W. Ke, L. Mao, C. C. Stoumpos, J. Hoffman, I. Spanopoulos, A. D. Mohite, M. G. Kanatzidis, *Adv. Energy Mater.* **2019**, *9*, 1803384.

[27] W. Fu, J. Wang, L. Zuo, K. Gao, F. Liu, D. S. Ginger, A. K. Y. Jen, *ACS Energy Lett.* **2018**, *3*, 2086.

[28] X. M. Lian, J. H. Chen, M. C. Qin, Y. Z. Zhang, S. X. Tian, X. H. Lu, G. Wu, H. Z. Chen, *Angew. Chem., Int. Ed.* **2019**, *58*, 9409.

[29] M. J. Yuan, L. N. Quan, R. Comin, G. Walters, R. Sabatini, O. Voznyy, S. Hoogland, Y. B. Zhao, E. M. Beauregard, P. Kanjanaboos, Z. H. Lu, D. H. Kim, E. H. Sargent, *Nat. Nanotechnol.* **2016**, *11*, 872.

[30] D. Giovanni, W. K. Chong, H. A. Dewi, K. Thirumal, I. Neogi, R. Ramesh, S. Mhaisalkar, N. Mathews, T. C. Sum, *Sci. Adv.* **2016**, *2*, e1600477.

[31] B. Cheng, T. Y. Li, P. C. Wei, J. Yin, K. T. Ho, J. R. D. Retamal, O. F. Mohammed, J. H. He, *Nat. Commun.* **2018**, *9*, 5196.

[32] W. Liu, J. Xing, J. Zhao, X. Wen, K. Wang, P. Lu, Q. Xiong, *Adv. Opt. Mater.* **2017**, *5*, 1601045.

[33] H. H. Zhang, Y. S. Wu, Q. Liao, Z. Y. Zhang, Y. P. Liu, Q. G. Gao, P. Liu, M. L. Li, J. N. Yao, H. B. Fu, *Angew. Chem., Int. Ed.* **2018**, *57*, 7748.

[34] F. Lédée, G. Trippé-Allard, H. Diab, P. Audebert, D. Garrot, J.-S. Lauret, E. Deleporte, *CrystEngComm* **2017**, *19*, 2598.

[35] W. Liu, X. Li, Y. Song, C. Zhang, X. Han, H. Long, B. Wang, K. Wang, P. Lu, *Adv. Funct. Mater.* **2018**, *28*, 1707550.

[36] R. W. Boyd, *Nonlinear Optics*, Academic Press, San Diego, CA **2008**.

[37] A. Hayat, A. Nevet, P. Ginzburg, M. Orenstein, *Semicond. Sci. Technol.* **2011**, *26*, 083001.

[38] X. Li, W. Liu, Y. Song, H. Long, K. Wang, B. Wang, P. Lu, *Nano Energy* **2020**, *68*, 104334.

[39] M. Anaya, J. F. Galisteo-Lopez, M. E. Calvo, J. P. Espinos, H. Miguez, *J. Phys. Chem. Lett.* **2018**, *9*, 3891.

[40] D. Lu, Y. Zhang, M. Lai, A. Lee, C. Xie, J. Lin, T. Lei, Z. Lin, C. S. Kley, J. Huang, E. Rabani, P. Yang, *Nano Lett.* **2018**, *18*, 6967.

[41] X. Fu, D. A. Jacobs, F. J. Beck, T. Duong, H. Shen, K. R. Catchpole, T. P. White, *Phys. Chem. Chem. Phys.* **2016**, *18*, 22557.

[42] H. H. Fang, S. Adjokatse, H. T. Wei, J. Yang, G. R. Blake, J. S. Huang, J. Even, M. A. Loi, *Sci. Adv.* **2016**, *2*, e1600534.

[43] W. K. Chong, K. Thirumal, D. Giovanni, T. W. Goh, X. F. Liu, N. Mathews, S. Mhaisalkar, T. C. Sum, *Phys. Chem. Chem. Phys.* **2016**, *18*, 14701.

[44] H. L. Shi, M. H. Du, *Phys. Rev. B* **2014**, *90*, 174103.

[45] C. Li, A. Guerrero, S. Huettner, J. Bisquert, *Nat. Commun.* **2018**, *9*, 5113.

[46] T. M. Koh, V. Shanmugam, J. Schlipf, L. Oesinghaus, P. Muller-Buschbaum, N. Ramakrishnan, V. Swamy, N. Mathews, P. P. Boix, S. G. Mhaisalkar, *Adv. Mater.* **2016**, *28*, 3653.

[47] R. L. Milot, R. J. Sutton, G. E. Eperon, A. A. Haghighirad, L. Martinez Hardigree, L. Miranda, H. J. Snaith, M. B. Johnston, L. M. Herz, *Nano Lett.* **2016**, *16*, 7001.

[48] Y. L. Song, C. Zhang, W. W. Liu, X. H. Li, H. Long, K. Wang, B. Wang, P. X. Lu, *Opt. Express* **2018**, *26*, 18448.